Research Article

LOW-DOSE LUTEOLIN FAILS TO MITIGATE DOXORUBICIN-INDUCED CARDIOVASCULAR AND PULMONARY INJURY IN RATS:

HISTOPATHOLOGICAL STUDY

Kübra SEVGİN[1] 🆔   *Yağmur ÇELİK[2]* 🆔
Nur ELAGÜL TOMBUL[3] 🆔   *Ayşe KÖSE VURUŞKAN[4]* 🆔

[1]*University of Health Sciences, Hamidiye International Faculty of Medicine, İstanbul*
[2]*University of Health Sciences, Institute of Health Sciences, İstanbul*
[3]*İstanbul Yeni Yüzyıl University, School of Medicine, İstanbul*
[4]*Carolinas Fertility Institute, Winston-Salem*

Article Info

ABSTRACT

This study aimed to evaluate the effect of luteolin (LUT) on lung, heart, and aorta histology in rats subjected to doxorubicin (DOX)-induced injury. Thirty-four 8-week-old male rats were divided to four groups: control (saline), LUT (20 µg/kg/day), DOX (5 mg/kg on days 1, 7, 14, 21, 28), and DOX+LUT (combined treatment). On day 29, rats were sacrificed for histological assessment of cardiovascular and pulmonary damage. Heart, lung, and aorta tissues were stained with Hematoxylin and Eosin (H&E), Toluidine Blue (TB), Safranin and Hemalum (SH), or Picrosirius Red (PSR). Semi-quantitative analyses of collagen and elastic fibers was performed using ImageJ. Group comparisons were made using one-way ANOVA with Bonferroni correction ($p < 0.0083$). DOX induced pronounced myocardial injury evidenced by loss of cross-striations, cytoplasmic vacuolization, coagulative necrosis, and an increase in collagen deposition with reduction in aortic elastic fibers and increase in aortic-collagen, as well as alveolar septal thickening, hemorrhage, and an increase in pulmonary mast cell density and interstitial collagen (all $p < 0.0083$). LUT treatment alone produced no histological alterations, and its co-administration at 20 µg/kg failed to ameliorate any of the DOX-induced changes. In conclusion, LUT (20 µg/kg) did not alleviate DOX-induced cardiopulmonary damage, underscoring the need for dose optimization in future studies.

INTRODUCTION

The anthracycline Doxorubicin (DOX) is a chemotherapeutic agent that has proven efficacious in the treatment of a range of neoplastic disorders, including leukemia, solid tumors, soft tissue sarcomas, and breast cancer (Malla, Prasad Niraula, Singh, Liou, & Kyung Sohng, 2010). However, despite its therapeutic benefits, the clinical use of DOX is significantly limited by its dose-dependent toxicity, particularly affecting the cardiovascular and pulmonary systems (Mitry & Edwards, 2016). DOX-induced cardiotoxicity is well-documented and often manifests as cardiomyopathy, arrhythmias, and heart failure. Additionally, pulmonary toxicity is a known adverse effect, presenting as interstitial pneumonitis and pulmonary fibrosis. Emerging

evidence also suggests that DOX can induce substantial structural and functional damage to the vascular system, including the aorta, contributing to systemic toxicity. This vascular injury is characterized by arterial stiffness and endothelial dysfunction, which may lead to long-term vascular impairment (Bosman et al., 2023). The mechanisms underlying these toxic effects are complex and multifactorial, involving oxidative stress, mitochondrial dysfunction, inflammation, and activation of apoptotic pathways (Songbo, Lang, Xinyong, Bin, Ping & Liang, 2019).

Luteolin (3′,4′,5′,7′-tetrahydroxyflavone, LUT) is a flavonoid present in several plant sources such as celery, parsley, and green peppers, has demonstrated promising protective effects in various models of oxidative stress and inflammation (Lv et al., 2025a). In particular, it has demonstrated a variety of pharmacological influences in both *in vivo* and *in vitro* studies, demonstrating antioxidant (Seelinger, Merfort, Wölfle & Schempp, 2008), anti-inflammatory (Xiong et al., 2024), anti-apoptotic (Han et al., 2023), and cardioprotective (Liu, Gao, Bu, & Zheng, 2022; Tongda, Li & Jiang, 2012) characteristics. It has been shown to demonstrate cardioprotective effects by modulating oxidative stress and inflammation by modulating Nrf2 and NF-κB pathways (L. Li et al., 2019) and by inhibiting hypoxia-activated calcium channels (Yan et al., 2019) in different cardiotoxicity models. Preclinical studies have demonstrated LUT's protective effects against DOX-induced liver and kidney toxicity by reducing oxidative and inflammatory stress (Owumi, Lewu, Arunsi & Oyelere, 2021). Additionally, LUT has been shown to attenuate DOX-induced cardiotoxicity through promoting mitochondrial autophagy and reducing oxidative stress (H. Xu et al., 2020).

Despite its presence in commercial health products, LUT is still in clinical trials for therapeutic use. Further research, including clinical studies and toxicity testing, is essential to support its safe and effective application (Lv et al., 2025b). In addition, despite these promising findings, the potential of LUT to mitigate DOX-induced damage across multiple organs, including the heart, lungs, and aorta, has not been comprehensively investigated. Moreover, existing studies predominantly focus on isolated organ systems, lacking integrated models that assess systemic toxicity.

To address this gap, the present study aimed to evaluate the histological effects of LUT on DOX-induced injury in the lung, heart, and aorta in a rat model. Through comprehensive histopathological analysis employing multiple staining techniques, this study aimed to assess the potential protective effects of LUT at a low dose (20 µg/kg) against DOX-induced cardiovascular and pulmonary toxicity, and to evaluate its efficacy as a multi-target protective agent in chemotherapy-associated tissue damage.

MATERIAL AND METHOD

Animals

In this study, male Sprague-Dawley rats were obtained from the Hamidiye Experimental Animal Production and Research Laboratory at Health Sciences University after approval from the Ethics Committee (Ethics Committee No: 2020-06/13). The rats were housed in a controlled environment with a 12-hour light/dark cycle and monitored daily. Rats were provided with standard pellets and water.

Experimental Groups

A total of 34 adult rats, aged 8 weeks, with a weight range of 90-150 g, were divided into four groups. The control group (n = 7) received 0.5 mL/day of normal saline intraperitoneally (i.p.) on days 1, 7, 14, 21, and 28. The LUT group (n = 9) received luteolin (LUT, Cayman Chemicals, USA) at a dose of 20 µg/kg for 28 days (Yahyazadeh & Altunkaynak, 2019). The DOX group (n = 9) received 5 mg/kg of doxorubicin hydrochloride (DOX, Cayman Chemicals) via intraperitoneal injection on days 1, 7, 14, 21, and 28. The DOX+LUT group (n = 9) received 5 mg/kg DOX i.p. on days 1, 7, 14, 21, and 28, along with 20 µg/kg LUT i.p. for 28 days as shown in Figure 1.
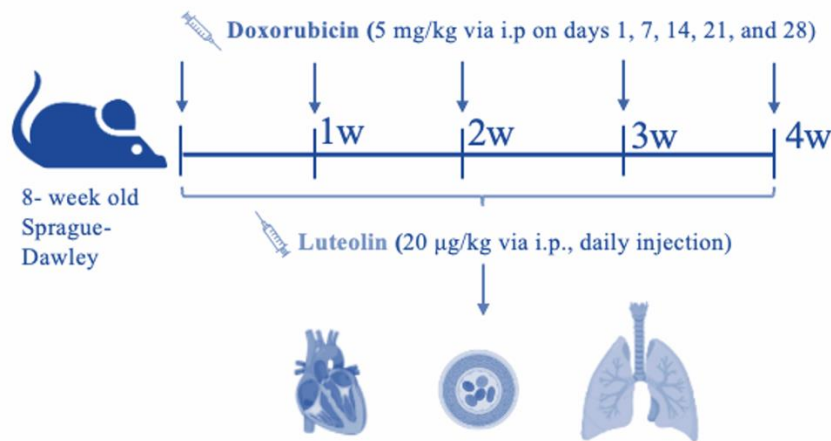

Figure 1. Experimental procedure

Sample Collection

The animals were euthanized 24 hours after the final injection by cervical dislocation under ketamine (75 mg/kg) and xylazine (10 mg/kg) anesthesia. The left lung, heart, and aorta were then fixed in formalin for subsequent histopathological examination.

Histological Processing

Following fixation, tissues were sequentially transferred into increasing concentrations of sucrose solutions (10%, 20%, and 30% w/v) prepared in PBS. The tissues were incubated in the sucrose solutions at 4°C for 24 hours each, or until they fully sank for cryoprotection. Then, tissues were embedded in optimal cutting temperature (OCT) compound (Thermo Fisher Scientific, USA), carefully placed in mold trays filled with OCT, and oriented as desired for sectioning. The OCT was then allowed to solidify at -80°C for at least 1 hour, ensuring the tissue samples were fully frozen and solidified. Embedded tissues were sectioned using a cryostat (Leica Microsystems, Germany) at a thickness of 10 μm on positively charged glass slides. After removing the OCT from the sections, the aorta, heart, and lung in each group were stained with Hematoxylin and Eosin (HE), Toluidine Blue (TB), and Safranin & Hemalum (SH) or picrosirius red (PSR).

Histopathological Assessment

Hematoxylin and Eosin Staining for Routine Tissue Morphologies

For Hematoxylin and Eosin (H&E) staining, sections were stained with Harris hematoxylin for 5 minutes, rinsed in running tap water, and differentiated in acid alcohol. After bluing in tap water, sections were counterstained with eosin for 1–2 minutes. Tissue morphology, changes in myocardial structure, cellular vacuolation, myofibrillar loss, necrosis, intermuscular edema, and areas of hemorrhage in heart tissue were examined (Wu et al., 2024). The vacuolization of smooth muscle cells in the tunica media of the aorta was examined to detect subtle structural changes in smooth muscles that may result from DOX-induced vascular toxicity. The alveolar hemorrhage and alveolar septal thickening in lung tissues were evaluated (Owumi et al., 2021b).

Picrosirius Red Staining for Collagen Distribution

The accumulation of collagen was examined in Picrosirius red (PSR)-stained heart (myocardial fibrosis), aorta (vascular fibrosis), and lung (pulmonary fibrosis) tissue sections. The heart, aorta, and lung sections (5 μm) were stained with 0.1% Sirius Red in saturated picric acid for 60 minutes, rinsed with 0.5% acetic acid, dehydrated, cleared, and mounted. Red-stained collagen fibers were visualized using a light microscope. Semi-quantitative analysis was performed in ImageJ by calculating the collagen-positive area (% of total area) in five random fields per section (Courtoy et al., 2020). The collagen area was quantified using ImageJ software (NIH, Bethesda, MD, USA) for a semi-quantitative assessment of fibrosis.

Safranin Staining for Elastic Fibers

Safranin and Hemalum (S&H) staining was performed to evaluate the elastic fibers in the medial layer of the vessel wall (Bosman et al., 2023b) to quantify vascular remodeling and structural damage caused by DOX. After rehydration, the preparations were stained with hemalum for 5 minutes. After rinsing, sections were stained with 0.1% Safranin O at 60° C overnight and then dehydrated, cleared, and mounted using entellan. Red elastic fibers were examined under the light microscope. Elastic fiber content was quantified by calculating the signal-to-wall area ratio (expressed as a percentage) with ImageJ software (Bosman et al., 2021).

Toluidine Blue Staining for Mast Cell Quantification

Toluidine Blue (TB) staining was performed to ascertain the alteration in the quantity of mast cells within the lung tissue after LUT treatment. Sections were stained with 0.1% Toluidine Blue solution (pH 2.0–2.5) for 2–3 minutes at room temperature, then briefly rinsed in distilled water. After dehydration through graded alcohols, sections were cleared in xylene and mounted. The quantification of mast cells was conducted in TB-stained lung sections, with 10 random areas from each preparation being assessed at 40X magnification. The numerical value of mast cells was expressed as the number of cells per unit area.

After staining the tissues, the preparations were examined with a Zeiss Scope A1 light microscope (Germany) equipped with a Zeiss Axiocam 105 Color digital camera (Germany).

Statistical Analysis

A Power Analysis was performed to determine the minimum number of experimental animals required (Type I error: 0.05; Power of test: 0.80) (Faul, Erdfelder, Buchner, & Lang, 2009). Statistical analysis was performed using GraphPad Prism 8.1.0 (GraphPad Inc., USA). Normality of the data distribution was assessed using the Shapiro-Wilk test. Comparisons between more than two groups were performed using one-way analysis of variance (ANOVA), followed by post hoc pairwise comparisons using the Bonferroni correction to adjust for multiple comparisons. A Bonferroni-adjusted p-value of <0.0083 (0.05/6) was considered statistically significant based on the number of pairwise comparisons among the four experimental groups.

RESULT

Figure 2 demonstrates histological analysis of the heart. Control (CONT) and LUT-only (LUT) groups maintained normal myocardial architecture, with tightly arranged

cardiomyocytes and no signs of structural disruption or fibrosis. On the other hand, histological analysis of longitudinal sections of the left ventricular myocardium revealed significant structural alterations, particularly in the DOX and DOX+LUT treatment groups. In the DOX-treated group, cardiomyocytes exhibited severe muscular damage characterized by disrupted cellular continuity, loss of cross-striations (red star), myocyte vacuolization (blue arrowhead), and hyper-eosinophilia of the sarcoplasm (dashed line). Many myocytes displayed small, dark pyknotic nuclei, indicative of early cell death. Intercellular spaces (black arrowhead) were widened, accompanied by interstitial edema (black arrowhead), and areas of hemorrhage (black star).
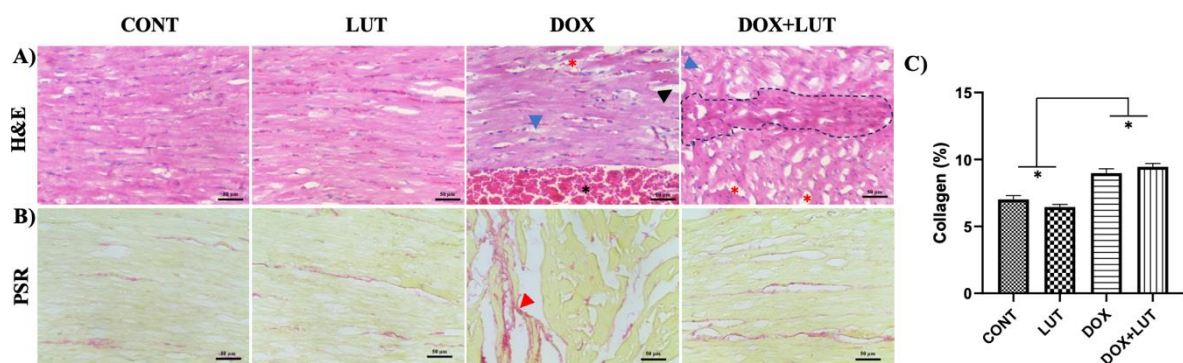

Figure 2. **A)** Representative H&E (**A**), and PSR (**B**) staining micrographs of longitudinal sections of left ventricular myocardium (×400; scale bar = 50 μm); blue arrowhead: cytoplasmic vacuolization, black arrowhead: intercellular spaces, black star: hemorrhage, red star: myofibrillar loss, dashed line: small foci of coagulative necrosis with hyper-eosinophilic myocyte sarcoplasm with small dark pyknotic nuclei, red arrowhead: collagen deposition. **C)** Semi-quantitative analysis of collagen deposition using ImageJ. Collagen-positive area (red color) was calculated as a percentage of total tissue area in five random fields per section (n=5). CONT: Control, LUT: Luteolin, DOX: Doxorubicin, DOX+LUT: Doxorubicin and Luteolin groups. H&E: Hematoxylin and Eosin, PSR: Picrosirius Red. *: p < 0.0083.

In the DOX+LUT group, heart sections showed notable disarray of cardiomyocytes, including a loss of the normal parallel alignment of cardiac muscle fibers. This group also displayed increased myofibrillar loss (red star) and focal areas of coagulative necrosis, identified by hyper-eosinophilic sarcoplasm and pycnotic nuclei (dashed line), similar to the early phases of necrosis seen in the DOX-only group. Cytoplasmic vacuolization (blue arrowhead) was also present, but without significant histological improvement over DOX treatment alone. DOX-treated groups (DOX and DOX+LUT) demonstrated significantly elevated collagen deposition (red arrowhead) compared to CONT and LUT groups in the PSR staining (p < 0.0083).
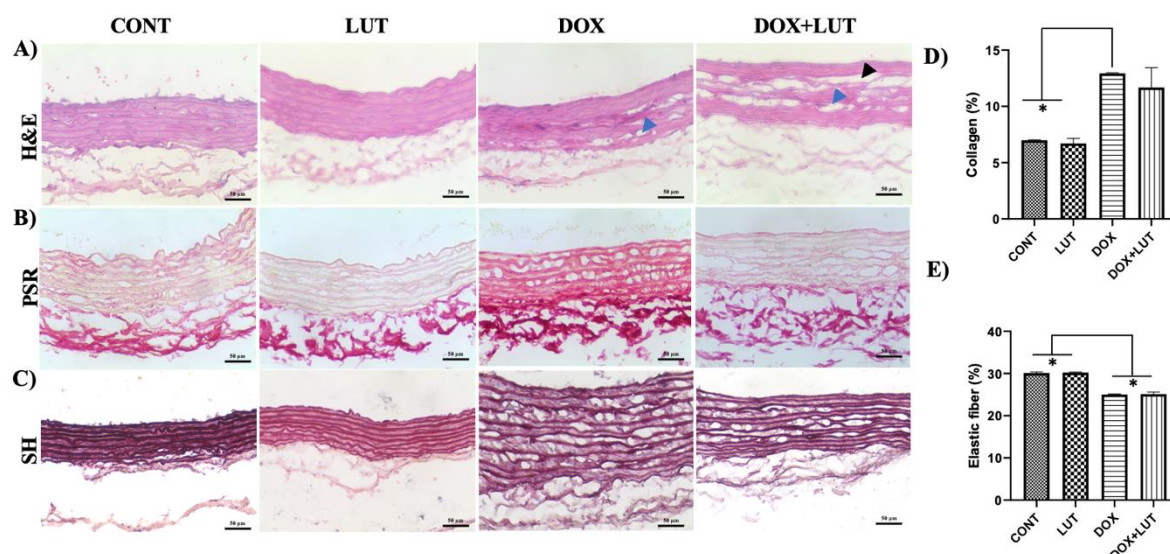
Figure 3. **A)** Representative H&E **(A)**, PSR **(B)**, and SH **(C)** staining micrographs of cross sections of aorta (×400; scale bar = 50 μm); blue arrowhead: cytoplasmic vacuolization, black arrowhead: intercellular spaces. Semi-quantitative analysis of collagen deposition **(D)** and elastic fibers **(E)** using ImageJ. Collagen-positive area (red color) and elastic fibers (brownish red color) were calculated as a percentage of total area in five random fields per section (n=5). CONT: Control, LUT: Luteolin, DOX: Doxorubicin, DOX+LUT: Doxorubicin and Luteolin groups. H&E: Hematoxylin and Eosin, PSR: Picrosirius Red. *: $p < 0.0083$.

Figure 3 presents histological analysis of the aorta. In the DOX group, several pathological changes are observed, including cytoplasmic vacuolization (blue arrowhead), increased intercellular spaces (black arrowhead). These changes were also present in the LUT and DOX+LUT groups. Compared with the CONT and LUT groups, both the DOX and DOX + LUT groups exhibited a reduced elastic fiber density, while the DOX group also demonstrated an increased collagen distribution ($p < 0.0083$).
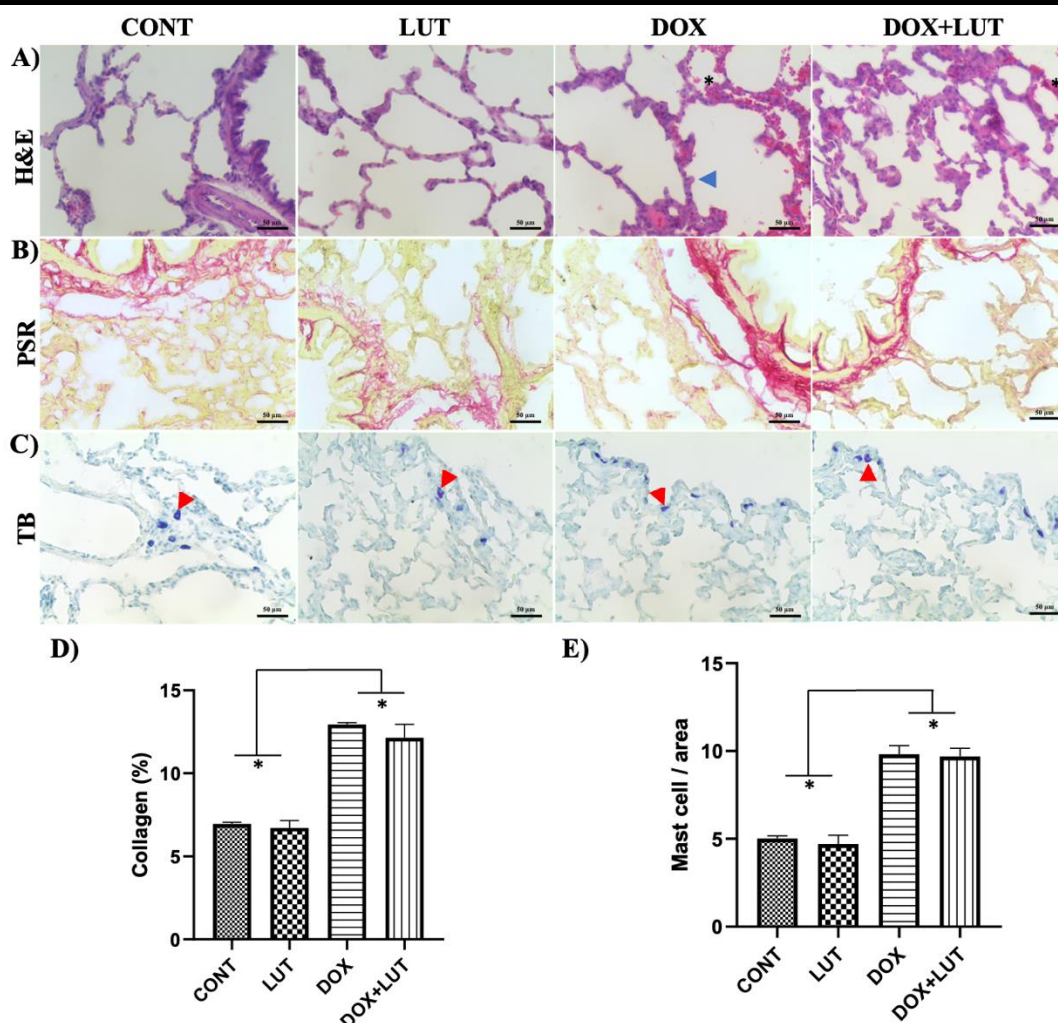
Figure 4. Representative H&E (**A**), PSR (**B**), and TB (**C**) staining micrographs of cross sections of lung (×400; scale bar = 50 µm); blue arrowhead: alveolar septal thickening, black star: hemorrhage, red arrowhead: mast cell. **D)** Semi-quantitative analysis of collagen deposition using ImageJ. Collagen-positive area (red color) was calculated as a percentage of total tissue area in five random fields per section (n=5). **E)** The quantification of mast cells was conducted in TB-stained lung sections. CONT: Control, LUT: Luteolin, DOX: Doxorubicin, DOX+LUT: Doxorubicin and Luteolin groups. H&E: Hematoxylin and Eosin, PSR: Picrosirius Red, TB: Toluidine Blue. *: p < 0.0083.

Figure 4 demonstrates histological assessments of lung tissue. In the DOX group, significant pathological features include alveolar septal thickening (blue arrowhead), hemorrhage (black star), and an increased presence of mast cells (red arrowhead). Compared with the CONT and LUT groups, both the DOX and DOX + LUT groups exhibited an elevated collagen distribution and mast cell amount per unit area (p < 0.0083).

DISCUSSION

This study evaluated the potential protective effect of luteolin (LUT) against doxorubicin (DOX)-induced cardiovascular and pulmonary toxicity. Histopathological analysis revealed that DOX caused significant tissue damage, including increased collagen deposition, reduced

aortic elastic fiber density, elevated alveolar septal thickening, hemorrhage, and mast cell counts. However, LUT at 20 µg/kg was insufficient to prevent these changes, indicating the need for further studies to optimize dosage and administration.

Inflammatory cytokines, mitochondrial dysfunction, oxidative stress pathways, intracellular calcium (Ca^{2+}) overload, iron-mediated free radical generation, as well as DNA and myocyte membrane damage are known to play pivotal roles in the pathogenesis of DOX-induced cardiotoxicity. Despite this complex pathophysiology, there are currently limited therapeutic options available for managing DOX-induced cardiotoxicity in clinical practice (Sheibani et al., 2022). This underscores the importance of exploring novel pharmacological strategies to prevent or attenuate DOX-related cardiac injury. In this study, despite its known antioxidant, anti-inflammatory, and anti-fibrotic effects (Lv et al., 2025b), low-dose LUT (20 µg/kg) failed to significantly mitigate DOX-induced myocardial damage. Collagen deposition remained elevated in the DOX+LUT group, indicating persistent cardiac fibrosis. These findings are consistent with previous reports showing that LUT's cardioprotective efficacy is dose-dependent, with higher doses more effectively reducing oxidative stress, inflammation, and fibrotic responses (Pan et al., 2025). Moreover, the complexity of DOX-induced cardiotoxicity, which involves mitochondrial dysfunction, ROS generation, apoptosis, and cytokine-mediated injury (Rawat, Jaiswal, Khurana, Bhatti & Navik, 2021), may limit the protective capacity of LUT alone. Combination therapies with other antioxidants or cardioprotective agents may be necessary to provide effective myocardial protection (Vincent, Ibrahim, Espey & Suzuki, 2013).

Anthracyclines induce oxidative stress through increased generation of reactive oxygen species, leading to vascular matrix remodeling and impaired endothelial-mediated regulation of smooth muscle tone, thereby increasing arterial stiffness. The associated endothelial dysfunction, characterized by reduced nitric oxide bioavailability and elevated pro-inflammatory cytokine expression, further exacerbates vascular injury (Chaosuwannakit et al., 2010). DOX has been reported to enhance Ca^{2+} release from the sarcoplasmic reticulum and promote Ca^{2+} entry in vascular smooth muscle cells (VSMCs), leading to increased VSMC contraction (Shen, Ye, C. L., Ye, K. H., Zhuang & Jiang, 2009). However, contradictory findings also exist, with other studies indicating that DOX reduces VSMC contraction by attenuating both Ca^{2+} release and entry (Gibson, Greufe, Hydock, & Hayward, 2013; Olukman et al., 2009). Although we did not evaluate molecular mechanisms in the present study, DOX administration was associated with significant collagen accumulation and a marked reduction in elastic fiber density, suggestive of vascular stiffening and remodeling (Bosman et al., 2021).

Cardiovascular studies have shown that LUT suppresses hypertensive aortic remodeling in the spontaneously hypertensive rat (Roberts et al., 2013), porcine coronary (Y. C. Xu et al., 2007), and relaxes rat coronary arterial smooth muscle cells via myocyte voltage-gated K^+ channels (W. Li et al., 2019). On the other hand, in this study LUT co-treatment did not significantly reverse these changes, suggesting limited efficacy in preventing vascular injury at the tested dose. This may be attributed to insufficient antioxidant and matrix-modulatory action at low concentrations. These results highlight the need for dose optimization or co-therapy strategies to mitigate DOX-induced vascular toxicity more effectively.

The administration of DOX has been demonstrated to induce an increase in collagen fibers within the lung alveolar wall, degeneration of certain cellular organelles, arterial endothelial and alveolar epithelial necrosis, edema, and emphysema in periarterial and subpleural regions (Yalçın et al., 2020). Similarly, DOX exposure induced severe pulmonary changes, including alveolar septal thickening, hemorrhage, increased collagen deposition, and elevated mast cell infiltration in this study. Several studies have been conducted in an attempt to mitigate the toxic effects of DOX on the lungs, including dosage optimization, chemopreventive agent and analogue synthesis, and their subsequent utilization (Injac et al., 2009). Previously, LUT's (50-100 mg/kg) protective effect against DOX-induced toxicity in the lungs and hematopoietic system of the rats was linked to its capacity to neutralize ROS/RNS, inhibit pro-apoptotic pathways, and reduce inflammatory responses (Owumi, Nwozo, Arunsi, Oyelere, & Odunola, 2021). However, we found that although LUT co-treatment slightly reduced collagen and mast cell levels, the effects were not statistically significant, indicating that low-dose LUT is insufficient to counteract the inflammatory and fibrotic responses induced by DOX in pulmonary tissue, resembling findings from prior studies advocating for higher or combined therapeutic interventions (Owumi et al., 2021b).

Although a similar dose of LUT (20 μg/kg) has been reported to mitigate the harmful effects of electromagnetic fields (Yahyazadeh & Altunkaynak, 2019) and DOX-induced testicular toxicity in rats (Elagül-Tombul, Söğüt, & Köse-Vuruşkan, 2024), we did not observe any significant protective effects in lung, aorta, or heart tissues in our study. This discrepancy may be due to tissue-specific sensitivity to DOX, differences in oxidative and inflammatory burden across organs. A key limitation of this study is the low LUT dose (20 μg/kg), which is substantially below the 10–50 mg/kg range commonly used to demonstrate anti-fibrotic and antioxidant effects. This sub-therapeutic dose may have been inadequate to counter DOX-induced fibrotic and oxidative damage, especially in cardiovascular and pulmonary tissues. The

absence of a clear protective effect in the DOX+LUT group may therefore reflect dose limitation rather than ineffectiveness of the compound itself. In addition, routine histological techniques were used in this study to assess tissue changes. While informative, they may overlook subtle molecular alterations. Future studies using immunohistochemistry or molecular analyses are needed to better understand the underlying mechanisms.

CONCLUSION

In conclusion, while LUT shows promise as a bioactive flavonoid, the current study demonstrates that low-dose administration provides limited protection against DOX-induced cardiopulmonary injury. Future studies should explore dose optimization, alternative delivery systems, or synergistic combinations to enhance its therapeutic potential.

Acknowledgements

REFERENCES

Bosman, M., Favere, K., Neutel, C. H. G., Jacobs, G., De Meyer, G. R. Y., Martinet, W., …Guns, P. J. D. F. (2021). Doxorubicin induces arterial stiffness: A comprehensive in vivo and ex vivo evaluation of vascular toxicity in mice. *Toxicology Letters*, 346. https://doi.org/10.1016/j.toxlet.2021.04.015

Bosman, M., Krüger, D., Van Assche, C., Boen, H., Neutel, C., Favere, K., … Guns, P. J. (2023). Doxorubicin-induced cardiovascular toxicity: a longitudinal evaluation of functional and molecular markers. *Cardiovascular Research*, 119(15). https://doi.org/10.1093/cvr/cvad136

Chaosuwannakit, N., D'Agostino, R., Hamilton, C. A., Lane, K. S., Ntim, W. O., Lawrence, J., …Hundley, W. G. (2010). Aortic Stiffness Increases Upon Receipt of Anthracycline Chemotherapy. *Journal of Clinical Oncology*, 28(1), 166–172. https://doi.org/10.1200/JCO.2009.23.8527

Courtoy, G. E., Leclercq, I., Froidure, A., Schiano, G., Morelle, J., Devuyst, … Bouzin, C. (2020). Digital image analysis of picrosirius red staining: A robust method for multi-organ fibrosis quantification and characterization. *Biomolecules*, *10*(11). https://doi.org/10.3390/biom10111585

Elagül-Tombul, N., Söğüt, İ., & Köse-Vuruşkan, A. (2024). An Examination of the Role of Luteolin in Doxorubicin-Induced Testicular Damage. *Journal of Evolutionary Biochemistry and Physiology*, *60*(3), 947–956. https://doi.org/10.1134/S0022093024030086

Faul, F., Erdfelder, E., Buchner, A., & Lang, A.-G. (2009). Statistical power analyses using G*Power 3.1: Tests for correlation and regression analyses. *Behavior Research Methods*, 41(4), 1149–1160. https://doi.org/10.3758/BRM.41.4.1149

Gibson, N. M., Greufe, S. E., Hydock, D. S., & Hayward, R. (2013). Doxorubicin-induced vascular dysfunction and its attenuation by exercise preconditioning. *Journal of Cardiovascular Pharmacology*, 62(4). https://doi.org/10.1097/FJC.0b013e31829c9993

Han, M., Lu, Y., Tao, Y., Zhang, X., Dai, C., Zhang, B., … Li, J. (2023). Luteolin Protects Pancreatic β Cells against Apoptosis through Regulation of Autophagy and ROS Clearance. *Pharmaceuticals*, 16(7). https://doi.org/10.3390/ph16070975

Injac, R., Radic, N., Govedarica, B., Perse, M., Cerar, A., Djordjevic, A., & Strukelj, B. (2009). Acute doxorubicin pulmotoxicity in rats with malignant neoplasm is effectively treated with fullerenol C60(OH)24 through inhibition of oxidative stress. *Pharmacological Reports*, 61(2), 335–342. https://doi.org/10.1016/S1734-1140(09)70041-6

Li, L., Luo, W., Qian, Y., Zhu, W., Qian, J., Li, J., … Liang, G. (2019). Luteolin protects against diabetic cardiomyopathy by inhibiting NF-κB-mediated inflammation and activating the Nrf2-mediated antioxidant responses. *Phytomedicine*, 59. https://doi.org/10.1016/j.phymed.2018.11.034

Li, W., Dong, M., Guo, P., Liu, Y., Jing, Y., Chen, R., & Zhang, M. (2019). Luteolin-induced coronary arterial relaxation involves activation of the myocyte voltage-gated K + channels and inward rectifier K + channels. *Life Sciences*, 221. https://doi.org/10.1016/j.lfs.2019.02.028

Liu, Z., Gao, S., Bu, Y., & Zheng, X. (2022). Luteolin Protects Cardiomyocytes Cells against Lipopolysaccharide-Induced Apoptosis and Inflammatory Damage by Modulating Nlrp3. *Yonsei Medical Journal*, 63(3). https://doi.org/10.3349/ymj.2022.63.3.220

Lv, J., Song, X., Luo, Z., Huang, D., Xiao, L., & Zou, K. (2025a). Luteolin: exploring its therapeutic potential and molecular mechanisms in pulmonary diseases. *Frontiers in Pharmacology*, 16. https://doi.org/10.3389/fphar.2025.1535555

Lv, J., Song, X., Luo, Z., Huang, D., Xiao, L., & Zou, K. (2025b). Luteolin: exploring its therapeutic potential and molecular mechanisms in pulmonary diseases. *Frontiers in Pharmacology*, 16. https://doi.org/10.3389/fphar.2025.1535555

Malla, S., Prasad Niraula, N., Singh, B., Liou, K., & Kyung Sohng, J. (2010). Limitations in doxorubicin production from Streptomyces peucetius. In *Microbiological Research* (Vol. 165, Issue 5). https://doi.org/10.1016/j.micres.2009.11.006

Mitry, M. A., & Edwards, J. G. (2016). Doxorubicin induced heart failure: Phenotype and molecular mechanisms. In *IJC Heart and Vasculature* (Vol. 10). https://doi.org/10.1016/j.ijcha.2015.11.004

Olukman, M., Can, C., Erol, A., Öktem, G., Oral, O., & Çinar, M. G. (2009). Reversal of doxorubicin-induced vascular dysfunction by resveratrol in rat thoracic aorta: Is there a possible role of nitric oxide synthase inhibition? *Anadolu Kardiyoloji Dergisi*, 9(4).

Owumi, S. E., Lewu, D. O., Arunsi, U. O., & Oyelere, A. K. (2021). Luteolin attenuates doxorubicin-induced derangements of liver and kidney by reducing oxidative and inflammatory stress to suppress apoptosis. *Human and Experimental Toxicology*, 40(10). https://doi.org/10.1177/09603271211006171

Owumi, S. E., Nwozo, S. O., Arunsi, U. O., Oyelere, A. K., & Odunola, O. A. (2021). Co-administration of Luteolin mitigated toxicity in rats' lungs associated with doxorubicin treatment. *Toxicology and Applied Pharmacology*, 411. https://doi.org/10.1016/j.taap.2020.115380

Pan, J., Chen, M.-Y., Jiang, C.-Y., Zhang, Z.-Y., Yan, J.-L., Meng, X.-F., … Qian, L.-B. (2025). Luteolin alleviates diabetic cardiac injury related to inhibiting SHP2/STAT3 pathway. *European Journal of Pharmacology*, 989, 177259. https://doi.org/10.1016/j.ejphar.2025.177259

Rawat, P. S., Jaiswal, A., Khurana, A., Bhatti, J. S., & Navik, U. (2021). Doxorubicin-induced cardiotoxicity: An update on the molecular mechanism and novel therapeutic strategies for effective management. In *Biomedicine and Pharmacotherapy* (Vol. 139). https://doi.org/10.1016/j.biopha.2021.111708

Roberts, R. E., Allen, S., Chang, A. P. Y., Henderson, H., Hobson, G. C., Karania, B., … Alexander, S. P. H. (2013). Distinct mechanisms of relaxation to bioactive components from chamomile species in porcine isolated blood vessels. *Toxicology and Applied Pharmacology*, 272(3). https://doi.org/10.1016/j.taap.2013.06.021

Seelinger, G., Merfort, I., Wölfle, U., & Schempp, C. M. (2008). Anti-carcinogenic effects of the flavonoid luteolin. In *Molecules* (Vol. 13, Issue 10). https://doi.org/10.3390/molecules13102628

Sheibani, M., Azizi, Y., Shayan, M., Nezamoleslami, S., Eslami, F., Farjoo, M. H., & Dehpour, A. R. (2022). Doxorubicin-Induced Cardiotoxicity: An Overview on Pre-clinical Therapeutic Approaches. In *Cardiovascular Toxicology* (Vol. 22, Issue 4). https://doi.org/10.1007/s12012-022-09721-1

Shen, B., Ye, C. L., Ye, K. H., Zhuang, L., & Jiang, J. H. (2009). Doxorubicin-induced vasomotion and [Ca2+](i) elevation in vascular smooth muscle cells from C57BL/6 mice. *Acta Pharmacologica Sinica*, 30(11). https://doi.org/10.1038/aps.2009.145

Songbo, M., Lang, H., Xinyong, C., Bin, X., Ping, Z., & Liang, S. (2019). Oxidative stress injury in doxorubicin-induced cardiotoxicity. *Toxicology Letters*, 307, 41–48. https://doi.org/10.1016/j.toxlet.2019.02.013

Tongda, X., Li, D., & Jiang, D. (2012). Targeting cell signaling and apoptotic pathways by luteolin: Cardioprotective role in rat cardiomyocytes following ischemia/reperfusion. In *Nutrients* (Vol. 4, Issue 12). https://doi.org/10.3390/nu4122008

Vincent, D. T., Ibrahim, Y. F., Espey, M. G., & Suzuki, Y. J. (2013). The role of antioxidants in the era of cardio-oncology. In *Cancer Chemotherapy and Pharmacology* (Vol. 72, Issue 6). https://doi.org/10.1007/s00280-013-2260-4

Xiong, L., Liu, Y., Wang, Y., Zhao, H., Song, X., Fan, W., … Zhang, Y. (2024). The protective effect of Lonicera japonica Thunb. against lipopolysaccharide-induced acute lung injury in mice: Modulation of inflammation, oxidative stress, and ferroptosis. *Journal of Ethnopharmacology*, 331, 118333. https://doi.org/10.1016/j.jep.2024.118333

Xu, H., Yu, W., Sun, S., Li, C., Zhang, Y., & Ren, J. (2020). Luteolin Attenuates Doxorubicin-Induced Cardiotoxicity Through Promoting Mitochondrial Autophagy. *Frontiers in Physiology*, 11. https://doi.org/10.3389/fphys.2020.00113

Xu, Y. C., Leung, S. W. S., Yeung, D. K. Y., Hu, L. H., Chen, G. H., Che, C. M., & Man, R. Y. K. (2007). Structure-activity relationships of flavonoids for vascular relaxation in porcine coronary artery. *Phytochemistry*, 68(8). https://doi.org/10.1016/j.phytochem.2007.02.013

Yahyazadeh, A., & Altunkaynak, B. Z. (2019). Protective effects of luteolin on rat testis following exposure to 900 MHz electromagnetic field. *Biotechnic and Histochemistry*, 94(4). https://doi.org/10.1080/10520295.2019.1566568

Yalçın, A., Türk, A., Aydın, H., Yılmaz, E., Çelik, İ. S., & Üçkardeş, F. (2020). Effects of Vitamin D on doxorubucin-induced lung injury and TRPM2 immunoreactivity in rats. *Journal of Surgery and Medicine*, 4(12). https://doi.org/10.28982/josam.842133

Yan, Q., Li, Y., Yan, J., Zhao, Y., Liu, Y., & Liu, S. (2019). Luteolin improves heart preservation through inhibiting hypoxia-dependent L-type calcium channels in cardiomyocytes. *Experimental and Therapeutic Medicine*. https://doi.org/10.3892/etm.2019.7214